Prediction of Solar Cycle 24

Using a Connectionist Model of the Emotional System

Mahboobeh Parsapoor[1,2], Urban Bilstrup[1], Bertil Svensson[1]
[1]School of Information Science, Computer and Electrical Engineering (IDE), Halmstad University, Halmstad, Sweden
[2]School of Computer Science, Faculty of Engineering & Physical Science, The University of Manchester, Manchester, UK.
[1]{Mahboobeh.Parsapoor, Urban.Bilstrup, Bertil.Svensson }@hh.se.
[2]mahboobeh.parsapoor@postgrad.manchester.ac.uk.

***Abstract*— Accurate prediction of solar activity as one aspect of space weather phenomena is essential to decrease the damage from these activities on the ground based communication, power grids, etc. Recently, the connectionist models of the brain such as neural networks and neuro-fuzzy methods have been proposed to forecast space weather phenomena; however, they have not been able to predict solar activity accurately. That has been a motivation for the development of the connectionist model of the brain; this paper aims to apply a connectionist model of the brain to accurately forecasting solar activity, in particular, solar cycle 24. The neuro-fuzzy method has been referred to as the brain emotional learning-based recurrent fuzzy system (BELRFS). BELRFS is tested for prediction of solar cycle 24, and the obtained results are compared with well-known neuro-fuzzy methods and neural networks as well as with physical-based methods.**

Keywords—*brain emotional learning-based recurrent fuzzy system, emotional system, solar activity forecasting,*

I. Introduction

Solar activity is a quasi-periodic space weather phenomenon that affects Earth's atmosphere which in turn causes harmful effects on space-based and ground-based communication systems such as satellites in low Earth orbit, high frequency radio communication systems and global positioning systems (GPS) [1]-[3]. To mitigate these adverse effects, alert systems for solar events have been developed. One central component of these alert systems is used to forecast solar activity by using records of solar activity indices such as sunspot numbers [3], [4]. Different types of neural networks, such as multilayer perceptron (MLP), weight elimination neural network (WNET) and local output gamma feedback neural network (LOGF-NN), along with various fuzzy and neuro-fuzzy models, have been tested to predict the maximum amplitude of the solar cycle using sunspot numbers[5]-[7].

The current cycle, Solar Cycle 24, began on January 10th 2008 and will last until 2018. This cycle is different from other cycles in three aspects: first, it has a 'long and deep minimum' [8], [9] (see Fig. 1); second, it has the smallest amplitude of any of the 10 past cycles (see Fig. 2); third, it has two peaks, the first in 2013 and the second, which is larger, in April 2014. Prediction of this solar cycle has captured much attention, and a comprehensive review of the predictions for this cycle by different methods is presented in [8]-[10].

In this paper, a new connectionist model that has been developed by taking inspiration from one of the emotional systems in mammalians is utilized to predict solar cycle 24. The connectionist model is based on the neural structure of fear conditioning [11], which is a mechanism by which a biological system learns fearful stimuli to predict aversive events. The model is referred to as the Brain Emotional Learning based Fuzzy Recurrent System (BELRFS) and was introduced in [12].

The rest of this paper is organized as follows. Section II gives a brief review of emotional learning in the brain and of the computational model of emotional learning. Section III describes the structure of BELRFS briefly. Section IV explains the Locally Linear Model Tree Learning Algorithm (LoLiMoT), which is used for comparison. Section V examines BELRFS to predict solar cycle 24. Section VI discusses notable conclusions.

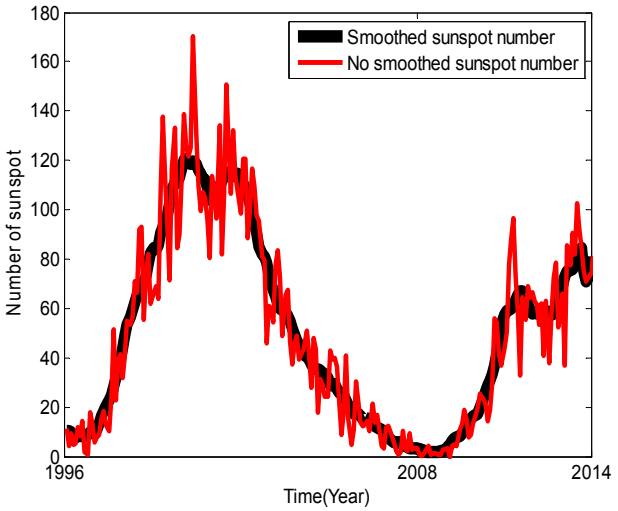

Fig. 1. The smoothed and non-smoothed sunspot numbers for solar cycle 23 and solar cycle 24.

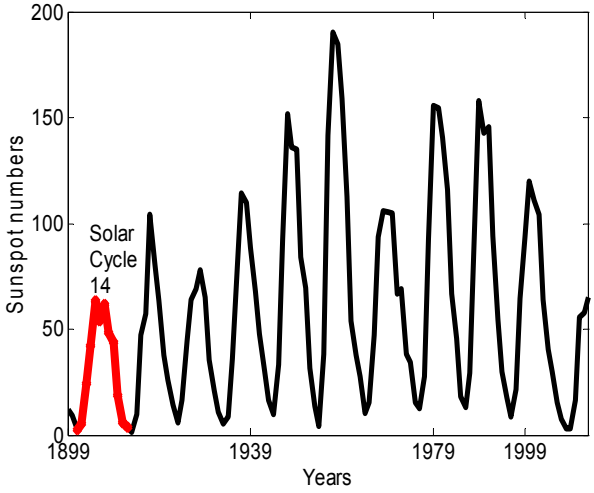

Fig. 2. The solar cycles from 1899 to 2014.

II. A REVIEW OF COMPUTATIONAL MODELS OF EMOTION

Computational models of emotion imitate aspects of emotion for specific purposes. A good example is a computational model that is called the amygdala-orbitofrontal system, it was introduced to simulate emotional learning in the brain. Computational models of emotions can be utilized to develop emotion-based decision-making models, emotion-based controllers, and emotion-based prediction models.

A. Three Applications of the Computational Model of Emotion

a) Emotion-based decision-making model: This model is the basis of the artificially intelligent (AI) emotional agent that integrates emotional reactions with rational reactions. EMAI (Emotionally Motivated Artificial Intelligence) was one of the first attempts to develop emotion-based agents. It was applied to simulate artificial soccer playing [13], and its results were fairly good. The Cathexis model [14] was another emotional agent developed to react to an environment by imitating an emotional decision-making process in humans. The model of the mind [15] was developed as a modular artificial agent to generate emotional behavior for making decisions. An agent architecture that called Emotion-based Robotic Agent Development (in reverse order, DARE) was developed on the basis of the somatic marker theory; it was tested in a multi-agent system and showed ability in modeling social and emotional behavior [16].

b)Emotion-based controller: The first practical implementation of an emotion-based controller is BELBIC (Brain Emotional Learning-Based Intelligent Controller) [17]. It was developed on the basis of Moren's and Balkenius' computational model [18]-[20]. The BELBIC has been successfully employed as an intelligent controller for controlling heating and air conditioning [21], of aerospace launch vehicles [22], intelligent washing machines [23], and trajectory tracking for stepper motors [24]. Another emotion-based intelligent controller is a neuro-fuzzy controller [25], which was integrated with emotion-based performance measurement to tune the parameters of the controller. Application of emotion-based controller in robotics was proposed in [26], which is an interesting example of applying emotional concepts in robotic applications and imitating the reinforcement learning aspect of emotional processing. The results of applying emotion-based controllers have shown that they have the capability to overcome uncertainty and complexity issues of control applications. Specifically, the BELBIC has been proven to outperform others in terms of simplicity, reliability, and stability [17], [21]-[24].

c) Emotion-based prediction models: Developing prediction models by imitating the emotional processing of the brain has captured the attention of researchers in the AI area. So far, some studies have been carried out to develop new neural networks by imitating some aspects of emotional learning. Good examples are the hippocampus-neocortex and amygdala hippocampus models, which have been proposed as neural network models [25], [26]. They combine associative neural networks with emotional learning concepts.

One type of emotion-based prediction models [27]-[36] can be referred to as brain emotional learning-based recurrent fuzzy system (BELRFS) that has been developed to predict the chaotic time series such as the Lorenz time series, sunspot numbers and auroral electrojet (AE) index [29].

B. A Computational Model of Emotional Learning

As was mentioned, the amygdala-orbitofrontal system is a type of computational model that has been defined to imitate emotional learning. It has a simple structure, which has been inherited from some parts of the limbic system (e.g., the amygdala, thalamus and sensory cortex). Its structure imitates the interaction between those parts of the limbic system and formulates the emotional response using mathematical equations [37]. The amygdala-orbitofrontal system consists of two subsystems: the amygdala and the orbitofrontal subsystems. Each subsystem has several nodes and receives a feedback signal (a reward). The model's output function has been defined as subtracting the orbitofrontal cortex's response from the amygdala's response. The learning rules aim to update the weights of the amygdala and the orbitofrontal subsystems. Due to its simplicity, it has been the basis of most controllers and prediction models inspired by emotional learning.

Figure 3 shows that the amygdala-orbitofrontal system consists of two main parts, the amygdala and the orbitofrontal cortex, and two accessory parts, the thalamus, and the sensory cortex. The interactions between the four parts of the model imitate the interactions between the parts of the brain that process emotional stimuli. The internal structure of each part of the model has been explained by the networking concept of a node [37], and the input, output, and function of each part are described below.

Thalamus: this is the first part of the system and is the part

that receives information and provides the coarse value of the information to send to the sensory cortex and the amygdala.

Sensory Cortex: this part receives information from the thalamus and sends this information to the amygdala and the orbitofrontal cortex.

Amygdala: this part receives input from the thalamus, the sensory cortex, and the orbitofrontal cortex. This part of the system consists of nodes, and each of which is labeled A, and the output of the amygdala is calculated as in (1).

$$\sum_i A_i \tag{1}$$

Orbitofrontal cortex: this part of the system receives inputs from the sensory cortex and the amygdala. It also consists of nodes, each node of which is labeled O. The output of the model is calculated as in (2).

$$\sum_i O_i \tag{2}$$

The final output, *E*, of the model is calculated as (3) [34].

$$E = \sum_i A_i - \sum_i O_i \tag{3}$$

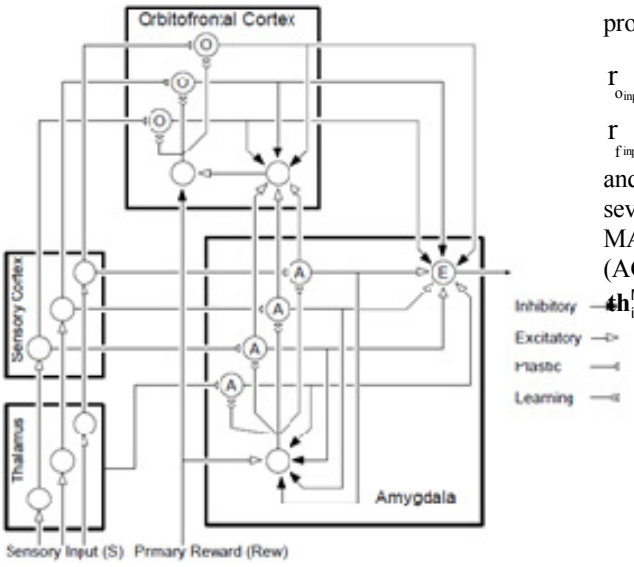

Fig. 3. The amygdala-orbitofrontal system (copied from [37] with permission). Receiving a sensory input as 'S' with three dimensions, the thalamus processes 'S' and sends its output to the amygdala, which consists of four nodes; the outputs of the amygdala are sent to the orbitofrontal cortex; this part consists of three nodes and receives another input from the sensory cortex. The output of the orbitofrontal cortex is sent to the 'E' node of the amygdala that is responsible for providing the final output of the amygdala-orbitofrontal system.

III. Brain Emotional Learning-based Recurrent Fuzzy System

The Brain Emotional Learning-based Recurrent Fuzzy System (BELRFS) is inspired by the neural structure of fear conditioning and have been developed as prediction and classification models [29]. This paper briefly explains the structural and functional aspects of BELRFS. Moreover, the learning algorithm of BELRFS is briefly described.

A. Structural and Functional Aspects of BELRFS

BELRFS consists of the following four main parts (see Fig. 4.(a)): the thalamus (TH), the sensory cortex (CX), the amygdala (AMYG), and the orbitofrontal cortex (ORBI). These parts imitate the connections between the thalamus, sensory cortex, amygdala, and orbitofrontal cortex, which are regions of the brain with roles in fear conditioning. The following steps explain how each part of BELRFS is connected to other parts. As Fig.4.(a) depicts, BELRFS receives an input as $\mathbf{i}_{input}$, from the training data set $\mathbf{I}_u = \{\mathbf{i}_{u,j}\}_{j=1}^{N_u}$, where N_u denotes the number of training samples and the subscript u is used to determine the input data that is chosen from the training data set. As the figure indicates TH is the first part to receive and process the input vector; AMYG is the final part to provide r_f as the output of BELRFS. Note that AMYG receives inputs from TH, CX and ORBI; AMYG provides $p^e_{a_{input}}$ and sends it to ORBI; while ORBI provides $r_{o_{input}}$ and sends it to AMYG, which is responsible for providing $r_{f_{input}}$. Figure 4 also describes the internal structure of BELRFS and its connections. As can be seen, each part consists of several internal sub parts; for example, TH is divided into MAX_MIN (MAXimum-MINimum) and AGG (AGGregation), which are responsible for providing $\mathbf{th}^{Max\_Min}_{input}$ and $\mathbf{th}^{AGG}_{input}$, respectively.

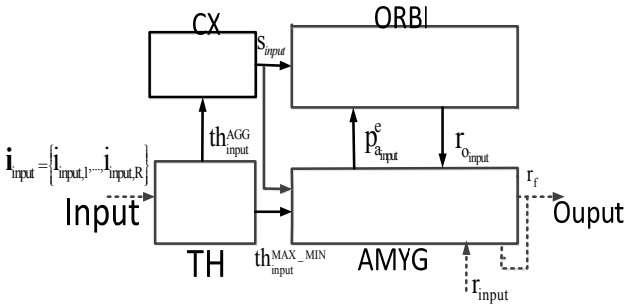

(a)

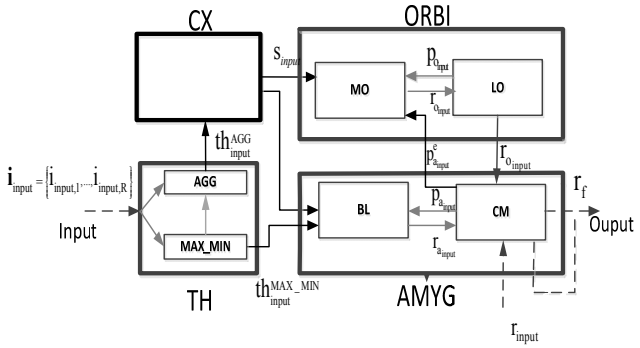

(b)

Fig .4. The structure of BELRFS (a). The outline structure of BELRFS and the connection between different parts; (b). The internal structure of BELRFS and its connections.

AMYG consists of two parts, BL and CM; BL represents the basal and lateral parts of the amygdala; while CM represents the accessory basal and the cortico-medial region of the amygdala. The BL is responsible for providing $\mathbf{r}_{a_{input}}$, while CM provides the final output $\mathbf{r}_{f}$. ORBI is also divided into two subparts, MO and LO, which respectively imitate the functionality of the medial and lateral parts of the orbitofrontal cortex. The function of each part by receiving $\mathbf{i}_{input}$ can be explained as the following:

1. TH receives $\mathbf{i}_{input}$, it consists of two parts that are named "MAX_MIN" (MAXimum_MINimum) and "AGG" (AGGregation). The function of these parts is implemented by the function of the assigned adaptive networks. Equations (4) and (5) calculate the functions of MAX_MIN and AGG that providing and respectively.

$$\mathbf{th}_{input}^{MAX\_MIN} = F_{AD}^{MAX\_MIN}(\mathbf{i}_{input}) \tag{4}$$

$$\mathbf{th}_{input}^{AGG} = F_{AD}^{AGG}(\mathbf{i}_{input}, \mathbf{th}_{input}^{Max\text{-}Min}) \tag{5}$$

Note that, the function of an adaptive network depends on the function of the adaptive nodes and the weights of the feed forward connections. The function of an adaptive network can be denoted as $F_{AD}(.)$.

2. CX receives $\mathbf{th}_{input}^{AGG}$ and provides $\mathbf{s}_{input}$ using an adaptive network whose function is calculated by (6). The output of CX, $\mathbf{s}_{input}$, is sent to the AMYG and ORBI.

$$\mathbf{s}_{input} = F_{AD}^{CX}(\mathbf{th}_{input}^{AGG}) \tag{6}$$

3. The AMYG receives $\mathbf{th}_{input}^{MAX\_MIN}$ and $\mathbf{s}_{input}$ from the TH and the CX, respectively. As was mentioned earlier, the AMYG consists of two parts that are named "BL" and "CM". The former is responsible for imitating the function of the basal and lateral parts of the amygdala; while CM is responsible for copying the function of the accessory basal and cortico-medial region of the amygdala [11]. The AMYG provides the primary output, $\mathbf{r}_{a_{input}}$,and the expected punishment, $\mathbf{p}^{e}_{a_{input}}$, that is sent to the ORBI (the subscript a is used to show the outputs of the AMYG). Similar to the other parts, the functionality of BL and CM are implemented using the functions of adaptive networks. Equation (7) calculates $\mathbf{r}_{a_{input}}$.

$$\mathbf{r}_{a_{input}} = F_{AD}^{BL}(\mathbf{th}_{input}^{MAX\_MIN}, \mathbf{s}_{input}) \tag{7}$$

4. The ORBI receives $\mathbf{s}_{input}$ and provides the secondary output, $\mathbf{r}_{o_{input}}$, using (8).

$$\mathbf{r}_{o_{input}} = F_{AD}^{ORBI}(\mathbf{s}_{input}) \tag{8}$$

5. Receiving $\mathbf{r}_{a_{input}}$ and $\mathbf{r}_{o_{input}}$, the AMYG provides the final output $\mathbf{r}_{f_{input}}$ (the subscript f has been used to show the final outputs) using (9).

$$\mathbf{r}_{f_{input}} = F_{AD}^{CM}(\mathbf{r}_{a_{input}}, \mathbf{r}_{o_{input}}) \tag{9}$$

B. Learning Aspect of BELRFS

The learning algorithm is a hybrid learning algorithm [38] that consists of Steepest Descent (SD) and Least Square Estimator (LSE). SD is utilized to update the parameters of adaptive nodes, while LSE is used to adjust the weights of the feed forward connections.

IV. LOCAL LINEAR MODEL TREE ALGORITHM

The Local Linear Model Tree algorithm (LoLiMoT) is a learning algorithm for local linear neuro-fuzzy model that is depicted by Fig. 5 [39]. The model has a neuro-fuzzy structure with one hidden layer, which consists of fuzzy neurons, and one linear output layer. The fuzzy neuron divides the input space into small subspaces using a locally linear model and a validity function, normalized Gaussian [39]. The output of the local linear model is calculated using (10), in which $U = [u_1, u_2 \ldots u_R]$ is the input vector of the model with R dimensions. The weights of a local linear node such as j can be considered as a vector $\boldsymbol{\omega} = [\omega_{j_0}, \omega_{j_1}, \ldots, \omega_{j_p}]$.

$$\hat{y}_j = \omega_{j_0} + \omega_{j_1} u_1 + \omega_{j_2} u_2 + \ldots + \omega_{j_p} u_R \tag{10}$$

The output of the model is calculated as the weighted summation of locally linear models by (11) [15], where $\varphi_j(\underline{u})$

is the validity function of each neuron, as calculated by (12), and $\mu_j(\underline{u})$ or $\mu_j(\underline{x})$ is the Gaussian function calculated by (13) [37]. Here, $\underline{x}$ is a subset of $\underline{u}$ that is sent to the nonlinear part of the node, while c_{jl} and σ_{jl} are parameters of the validity function.

$$\hat{y} = \sum_{j=1}^{M} \hat{y}_j \varphi_j(\underline{u}) \tag{11}$$

$$\varphi_j(\underline{u}) = \mu_j(\underline{u}) \Big/ \sum_{j=1}^{M} \mu_j(\underline{u}) \tag{12}$$

$$\mu_j(\underline{x}) = \exp\left(\frac{-1}{2}\left(\frac{(x_1 - c_{j1})^2}{\sigma_{j1}^{\ 2}}\right)\times\ldots\right.$$
$$\left.\times\exp\left(\frac{-1}{2}\left(\frac{(x_R - c_{jR})^2}{\sigma_{jR}^{\ 2}}\right)\right)\right. \tag{13}$$

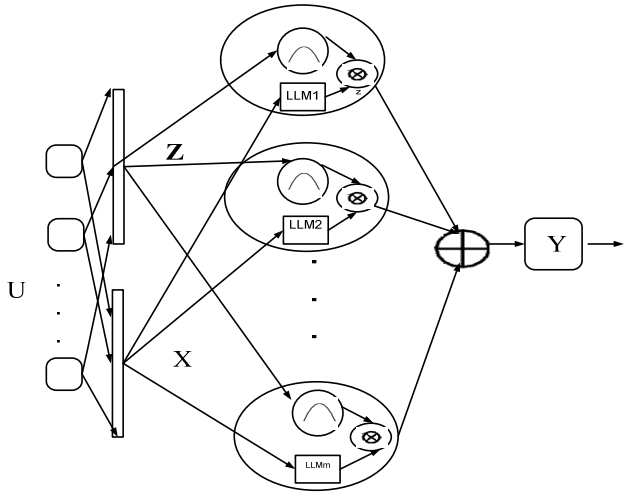

Fig. 5. The structure of LoLiMoT.

The learning parameters of the model are classified into the linear parameters (the weighs in equation (10)), the local linear model parameters and nonlinear parameters, which correspond to validity functions. A global optimization method based on the least squares method is utilized to optimize the $M(R+1)$ linear learning parameters [39]. Here, M is the number of fuzzy neurons of the hidden layer and R is the dimension of the input vector. The least squares method updates the vector of the linear parameters, W, that is described by (14) [39].

$$W = [\omega_{l_0}, \ldots, \omega_{l_R}, \omega_{2_0} \ldots, \omega_{2_R}, \ldots, \omega_{M_0}, \ldots, \omega_{M_R}] \tag{14}$$

The updating rules are formulated in (15) while the output of the model is calculated in (16), in these, X is a matrix of X_j as given by (17), and each X_j is a matrix of corresponding validation functions to the local neuron j as (18) [1] and [15], $\underline{y}$ and $\hat{y}$ are the target output and the obtained output, respectively.

$$\underline{\hat{W}} = (\underline{X}^T X)^{-1} \underline{X}^T \underline{y} \tag{15}$$

$$\underline{\hat{y}} = \underline{X}.\hat{W} \tag{16}$$

$$X = \left[X_1, .., X_j, ..., X_M\right] \tag{17}$$

$$X_j = \begin{bmatrix} \varphi_j(\mathbf{u}(1)), u_1(1)\varphi_j(\mathbf{u}(1)), ..., u_R(1)\varphi_j(\mathbf{u}(1)) \\ .... \\ \varphi_j(\mathbf{u}(N_u)), u_1(N_u)\varphi_j(\mathbf{u}(N_u)), ..., u_R(N_u)\varphi_j(\mathbf{u}(N_u)) \end{bmatrix} \tag{18}$$

To optimize the learning parameters, which are divided into the linear and nonlinear parameters, the local linear model tree algorithm (LoLiMoT) is applied. This algorithm, which is an incremental heuristic algorithm, consists of two loops. The first loop updates the nonlinear parameters and the nested loop optimizes the linear parameters. The following steps explain LoLiMoT [39]:

1) An initial model is selected and considered as the starting point for the algorithm. Starting with M=1 means that the initial model has one neuron in the hidden layer.

2) The local cost function, which is formulated in (19), is calculated for each neuron. The worst local linear model (LLM) that has a maximum value of the loss function is selected and indicated by l, where $e^2(.)$ is the absolute error.

$$I_j = \sum_{input=1}^{N_u} e^2(input)\varphi_j\left(\underline{u}(input)\right) \tag{19}$$

3) The loss function is calculated for all possible divisions of l. The best one, the partition that has a minimum value for the loss function, is selected and indicated by k.

4) The validity function that corresponds to k is added and the number of locally linear models is increased by one.

5) The algorithm is stopped if the termination condition is satisfied, otherwise it goes to step 2 and continues.

The main preference of LoLiMoT is its low time complexity because of its linear growth with the number of fuzzy neurons.

V. EVALUATION OF BELRFS

As mentioned, this paper compares the results obtained from applying BELRFS and LoLiMoT to predict solar cycle 24. To do so, the normalized mean square error (NMSE), which is given in (20), is utilized to measure the performance

of the prediction models. Here $r_{f\,input}$ and r_{input} refer to the predicted values and desired values, respectively. The parameter $\bar{r}_{input}$ is the average of the desired values.

$$NMSE = \sum_{input=1}^{N_u} (r_{f\,input} - r_{input})^2 \Big/ \sum_{input=1}^{N_u} (r_{input} - \bar{r}_{input})^2 \qquad (20)$$

The first experiment is the non-smoothed monthly sunspot numbers [41] from 1700 until April 1996. It is used to train the BELRFS and LoLiMoT, models that are then tested by using them to predict a part of solar cycle 23 and solar cycle 24 one, five and ten months in advance. Note that during solar cycle 24, there are two peak values for the (non-smoothed) monthly sunspot numbers. The first is at 96.7 and the second is at 102.3. The NMSEs obtained and the predicted values of the first and second peaks of solar cycle 24 are listed in Table I, showing that both BELRFS and LoLiMoT have similar results in terms of NMSEs. The maximum absolute errors for LoLiMoT and BELRFS are 16 and 19 respectively (these are related to the ten-month ahead prediction of the second peak). Hence, it can be concluded that for long-term prediction, LoLiMoT performs better than BELRFS. Fig. 6 describes the values predicted by BELRFS and LoLiMoT versus the real values of monthly sunspot numbers from May 1996 to September 2014 (parts of solar cycle 23 and 24). As Fig. 6 shows, BELRFS is slightly better than LoLiMoT in predicting the first peak. The predicted value of the first peak obtained by BELRFS is 87.8 while LoLiMoT predicts that the first peak is 90.57.

TABLE I. COMPARISON BETWEEN BELRFS LOLIMOT PREDICTIONS OF SOLAR CYCLES WITH NON-SMOOTHED MONTHLY SUNSPOT NUMBERS.

Learning Method	**Characteristics of prediction**		
	Prediction horizon (month in advance)	Predicted Values of First and Second peak	NMSE
BELRFS	One month	First peak=87.8 Second peak=95.38	1.330e-1
BELRFS	Five month	First peak=72.15 Second peak=108.32	2.694e-1
BELRFS	Ten month	First peak=91.97 Second peak=121	3.32e-1
LoLiMoT	One month	First peak=90.57 Second peak=95.6	1.325e-1
LoLiMoT	Five month	First peak=111 Second peak=91.9	2.732e-1
LoLiMoT	Ten month	First peak=96.98 Second peak=118.1	3.487e-1
Real Values	----------	First peak=96.7 Second peak=102.3	----------

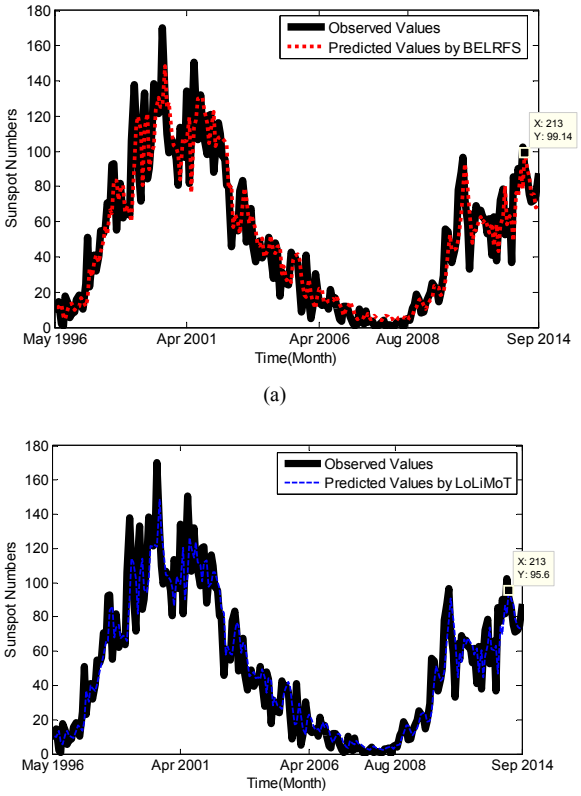

Fig. 5. The one month in advance values predicted of solar cycle 23 and solar cycle 24 (a). The red dotted lines show the values predicted by BELRFS. (b) The blue dashed line shows the values predicted by LoLiMoT.

In the second experiment, the smoothed monthly sunspot time series from March 1996 to September 2014 is recursively predicted by BELRFS and LoLiMoT. Hence, the monthly sunspot numbers from 1700 until 1975 are considered as training data. And the sunspot numbers from January 1976 to April 1996 are predicted (the step of prediction is one month ahead) by both methods. These predicted values without any correction due to the observed values, are then added to the training data and the monthly sunspots from March 1996 to September 2014, which are parts of solar cycles 23 and 24, are predicted. Note that during solar cycle 24, the smoothed monthly sunspot numbers have shown two peak values, the first at 66.9 during the second at 87.6. The graphs in Fig. 6 show the recursively predicted values by BELRFS and LoLiMoT. It can be observed that the performance of BELRFS is similar to the one of LoLiMoT. Table II compares BELRFS and LoLiMoT regarding the predicted values and times of occurrence of the two peaks during this cycle. As both Table II and Fig. 6 show, the results obtained by BELRFS are close to those obtained by LoLiMoT, which is considered a powerful prediction model [5]. Thus, BELRFS, which is model inspired by the emotional system, can also be utilized as a chaotic time series predictor and performs similarly to LoLiMoT.

TABLE II. COMPARISON BETWEEN LOLIMOT AND BELRFS IN PREDICTING SOLAR CYCLE 24.

Learning Method	Characteristics of prediction		
	NMSE	First Peak	Second Peak
BELRFS	0.002	68.16	88.17
LoLiMoT	0.0019	67.73	88.29
Real values	-----	66.9	87.6

As discussed earlier, prediction of solar cycle 24 has captured a lot of attention, and various space weather centers and research groups [42] have made efforts to predict the maximum amplitude of this cycle and the time of occurrence during this cycle. Table III lists different neuro-fuzzy methods and neural networks that have been applied to predicting this cycle. The interesting point is that none of them had predicted the second peak of the cycle. It should be noted that this table just aims to present the attempts that have done to predict solar cycle 24. In order to compare the performance of BELRFS with these methods, the similar training and test data sets should be considered. **observed value**

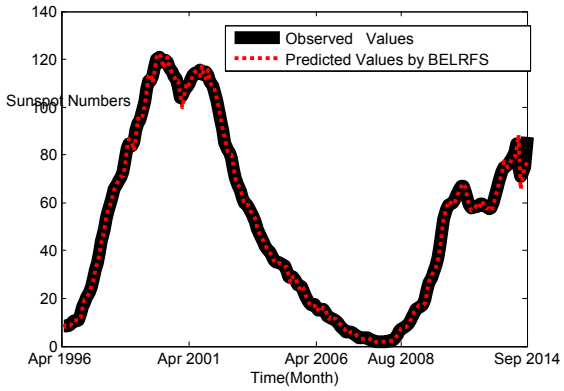

(a)

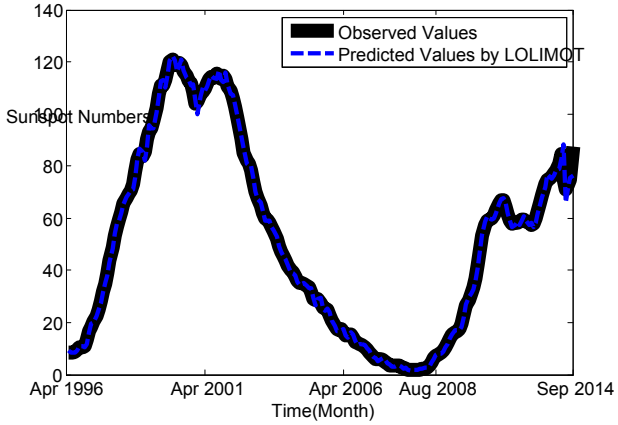

(b)

Fig.6.(a). Recursively predicted values, one-month ahead, for smoothed monthly sunspot numbers from May 1996 to September 2014 using BELRFS.(b). Recursively predicted values, one-month ahead, for smoothed monthly sunspots from May 1996 to September 2014 using LoLiMoT.

TABLE III. PRESENTING DIFFERENT METHODS FOR PREDICTING SOLAR CYCLE 24

Methods	Characteristics of Methods		
	Peak Values (first, second)	Peak Time(first, second)	Reference
BELRFS	First peak=87.8 Second peak=95.38	First time =2013 Second time=2014	this paper
LoLiMoT	First=90.57 Second=95.6	First time =2013 Second time=2014	this paper
Neural Network	First=65±13 Second=NA	First time =2013 Second time=NA	[43]
Neural Network	First=145 Second=NA	First time =2009 Second time=NA	[44]
Neuro-fuzzy Methods	First=145 Second=NA	First time =2011-2012 Second time=NA	[45]
Neuro-fuzzy Methods	First=101±8 Second=NA	First time =2013 Second time=NA	[46]
Observed values	First= 72 Second= 81.9	First time =2013 Second time=2014	[40]

VI. CONCLUSION

This paper applied BELRFS to be used as a prediction model of solar cycle 24. The performance of this model has been evaluated by testing it on solar cycle 24. The results obtained have shown that this model is as accurate a prediction model as LoLiMoT. Hence, BELRFS can be considered as a solar activity forecasting model with a good performance. In addition it is possible to modify it to provide a more accurate prediction model. In future work, BELRFS will also be applied to the prediction of geomagnetic storms.

ACKNOWLEDGEMENTS

The first author, Mahboobeh Parsapoor, would like to offer her sincerest thanks to the late Professor Caro Lucas for his inspiration and kind support in supervising her research process concerning the development of the brain emotional learning-inspired models. In addition, the first author is grateful to Dr. John Brooke to suggest applying the machine learning methods on solar cycle 24. The authors are thankful to National Oceanic and Atmospheric Administration National Weather Service Space Weather Prediction Center and Royal Observatory of Belgium for providing the sunspot number data set.

REFERENCES

[1] D.H. Hathaway, "The solar cycle,"in *Living Rev. Sol. Phys*. 7, 1, 2010.

[2] K. Schatten, "Solar Activity and The Solar Cycle," in *Adv. Space Res*, 32(4), pp.451,2003.

[3] J. A. Joselyn, J. B. Anderson, H. C. Coffey, K. Harvey, D. Hathaway, G. Heckman, E. Hildner, W. Mende, K. Schatten, R. Thompson, A. W. P. Thompson, and O. R. White, "Panel achieves consensus prediction of solar cycle 23", *Eos Trans. AGU*, vol. 78, pp.211 -212, 1997.

[4] K. Petrovay, "Solar Cycle Prediction", *Living Rev. Solar Phys*. **7**, pp.6,2010.

[5] A. Golipour, B. N.Araabi., C. Lucas, "Predicting Chaotic Time Series Using Neuraland Neurofuzzy Models A Comparative Study,'' *J. Neural. Process Lett.,* vol. 24, no. 3, pp. 217-239, 2006.

[6] A. Golipour, C. Lucas and D.shamirzadi, “Purposeful prediction Of Space Weather Phenomena by Simulated Emotional Learning,’’ *modeling Journal,* vol. 24, pp. 65-72, 2004.

[7] M. Mirmomeni, E. Kamaliha, E, M. Shafiee and C.Lucas, “Long-term prediction of solar and geomagnetic activity daily time series using singular spectrum analysis and fuzzy descriptor models,’’ *J. Earth Planets Space*, J. *Space,* Vol.61, pp.1089 –1101, 201.

[8] Hathaway, D. H.*,* R. M. Wilson*, and* E. J. Reichmann, *“*A synthesis of solar cycle prediction techniques*,”* in *J. Geophys. Res.,* 104*(*A10*), pp.* 22375–22388*,1999. doi:*10.1029/1999JA900313

[9] http://solarscience.msfc.nasa.gov/predict.shtml

[10] http://www.noaa.gov/features/economic_0708/spaceweather.html

[11] J.E.Ledoux, *The emotional brain: the mysterious underpinnings of emotional life,* Simon & Schuster, NY, 1998.

[12] M. Parsapoor, M, U. Bilstrup, "Neuro-fuzzy models, BELRFS and LoLiMoT, for prediction of chaotic time series," in *Proc. IEEE Int. Conf. INISTA.,* pp.1-5, 2012.

[13] Damas, B. D. and Custódio, L.: "Emotion-Based Decision and Learning Using Associative Memory and Statistical Estimation," *J. Informatica (Slovenia),* vol. 27, no. 2, pp. 145-156, 2004.

[14] J. D. Velásquez., “When Robots Weep: Emotional Memories and Decision-Making,” in *Proc. Conf. on Artificial Intelligence*, pp.70-75. 1997.

[15] S.H. Zadeh, S. B. Shouraki, and R. Halavati, R. “Emotional behavior: A resource management approach,” *J. Adaptive Behavior, vol.* 14, pp. 357-380, 2006.

[16] M. Maçãs and L. Custódio, "Multiple Emotion-Based Agents Using an Extension of DARE Architecture," *J. Informatics (Slovenia),* vol. 27, no. 2, pp. 185-196, 2004.

[17] C. Lucas, D. Shahmirzadi, N. Sheikholeslami, “Introducing BELBIC: brain emotional learning based intelligent controller,’’ *J. INTELL. AUTOM. SOFT. COMPUT.,* vol. 10, no. 1, pp. 11-22, 2004.

[18] E. Daryabeigi, G. R. A. Markadeh, C. Lucas,"Emotional controller (BELBIC) for electric drives — A review," in *Proc. Annual Conference on IEEE Industrial Electronics,* pp.2901-2907, *2010,*.

[19] N. Sheikholeslami, D. Shahmirzadi, E. Semsar, C. Lucas., "Applying Brain Emotional Learning Algorithm for Multivariable Control of HVAC Systems,", *J. INTELL. FUZZY. SYST.*vol.16, pp. 1–12, 2005.

[20] *A. R. Mehrabian, C. Lucas, J. Roshanian,"Aerospace Launch Vehicle Control: An Intelligent Adaptive Approach," J. Aerosp. Sci. Technol*.,vol.10,pp. 149–155, 2006..

[21] *R. M. Milasi, C. Lucas, B. N. Araabi, "Intelligent Modeling and Control of Washing Machines Using LLNF Modeling and Modified BELBIC,"* in *Proc. Int. Conf. Control and Automation.,* pp.812-817, 2005,.

[22] A. M. Yazdani1, S. Buyamin1, S. Mahmoudzadeh2, Z. Ibrahim1 and M. F. Rahmat1., “Brain emotional learning based intelligent controller for stepper motor trajectory tracking,” *J. IJPS*., vol. 7, no. 15, pp. 2364-2386, 2012.

[23] M. Fatourechi, C. Lucas, and A.K. Sedigh, "Emotional Learning as a New Tool for Development of Agent-based System," *J. Informatics (Slovenia),* vol. 27, no. 2, pp.137-144., 2004.

[24] S. C. Gadanho, L. Custódio: “Learning Behavior-selection in a Multi-goal Robot Task,” *J. Informatics (Slovenia), vol. 27*, no. 2, pp. 175-184, 2003.

[25] T. Kuremoto, T. Ohta, K., Kobayashi, M., Obayashi, “A dynamic associative memory system by adopting amygdala model,” J. *AROB, v*ol.13, pp.478–482, 2009.

[26] T. Kuremoto, T. Ohta, K. Kobayashi, K., *M.* Obayashi, “A functional model of limbic system of brain,” in *Proc. Int. Conf. Brain informatics*, pp.135-146, 2009.

[27] M. Parsapoor, U. Bilstrup, "Brain Emotional Learning Based Fuzzy Inference System (BELFIS) for Solar Activity Forecasting," in *Proc. IEEE Int. Conf. ICTAI 2012*, 2012.

[28] M. Parsapoor and U. Bilstrup, “Chaotic Time Series Prediction Using Brain Emotional Learning Based Recurrent Fuzzy System (BELRFS),” in *International Journal of Reasoning-based Intelligent Systems*, Vol.5, No.2, pp.113 – 126,2013.

[29] M. Parsapoor, “*Brain Emotional Learning-Inspired Models. Licentiate Dissertation”*, Halmstad University, 2014.

[30] M. Parsapoor, U. Bilstrup, "Brain emotional learning based fuzzy inference system (Modified using radial basis function)," *Digital Information Management (ICDIM), 2013 Eighth International Conference on*, vol., no., pp.206,211, 10-12 Sept. 2013, doi: 10.1109/ICDIM.2013.6693994.

[31] M. Parsapoor, C. Lucas, "Predicting of Solar Geomagnetic Indices by Utilizing the Emotional Learning Method," *in Proc. Int. Conf. FORGES 2008,doi: 10.13140/RG.2.1.4854.4165*.

[32] M. Parsapoor, U. Bilstrup, B. Svensson, "A Brain Emotional Learning-based Prediction Model for the prediction of geomagnetic storms," *Computer Science and Information Systems (FedCSIS), 2014 Federated Conference on* , vol., no., pp.35,42, 7-10 Sept. 2014.

[33] M. Parsapoor, U. Bilstrup, B. Svensson, "Neuro-fuzzy models for geomagnetic storms prediction: Using the auroral electrojet index," *Natural Computation (ICNC), 2014 10th International Conference on* , vol., no., pp.12,17, 19-21 Aug. 2014.

[34] M. Parsapoor, J. Brooke and B. Svensson, “A New Computational Intelligence Model for Long-Term Prediction of Solar and Geomagnetic Activity”,*Twenty-Ninth AAAI Conference on Artificial Intelligence*, pp. 4192-4193, Jan 2015.

[35] M. Parsapoor, C. Lucas, “Modifying Brain Emotional Learning Model for Adaptive Prediction of Chaotic Systems with Few Data Training Samples" *in Proc. Int. Conf. ICAOR. pp. 328-341, 2008*, DOI: 10.13140/RG.2.1.1118.8648.

[36] M. Pasrapoor, U. Bilstrup, "An emotional learning-inspired ensemble classifier (ELiEC)," *Computer Science and Information Systems (FedCSIS), 2013 Federated Conference on* , vol., no., pp.137,141, 8-11 Sept. 2013.

[37] J.Moren, C.Balkenius,“A computational model of emotional learning in the amygdala,’’, in *From Animals to Animates*, MIT, Cambridge, 2000.

[38] R. Jang, C. Sun and E. Mizutani, Neuro-Fuzzy and Soft Computing: A Computational Approach to Learning and Machine Intelligence. Upper Saddle River, NJ: Prentice Hall, 1997.

[39] O. Nelles, Nonlinear System Identification: From Classical Approaches to Neural Networks and Fuzzy Models. Berlin, Germany: Springer-Verlag, 2001.

[40] http://solarscience.msfc.nasa.gov/predict.shtml

[41] SILSO data/image, Royal Observatory of Belgium, Brussel.

[42] W.D. Pesnell, “Predictions of Solar Cycle 24”, *Solar Phys*., vol. 252, pp. 209–220, 2008.

[43] A. Ajabshirizadeh, N. M. Jouzdani and Abbassi, *Research in Astronomy and Astrophysics*, vol. 11, pp. 491-496, 2011.

[44] G. Maris and A. Oncica, “Solar cycle 24 forecasts,” *Sun & Geospace*, 1, 2006.

[45] A. Attia, H. Ismail, H. Basurah, Astrophys. *Space Sci*. 344, pp. 5, 2013.

[46] A. Gholipour, C. Lucasa, B. N. Araabia, and M. Shafiee, “Solar activity forecast: Spectral analysisand neurofuzzy prediction,” *J. Atm. Sol.-Terr. Physics*, 67, 595–603, 2005.